THE JOURNAL OF NAVIGATION (2016), **69**, 639–658.
doi:10.1017/S037346331500082X

Asynchronous Pseudolite Navigation Using C/N_0 Measurements

Daniele Borio, Ciro Gioia and Gianmarco Baldini

(*European Commission, Joint Research Centre* (*JRC*)*, Institute for the Protection and Security of the Citizen* (*IPSC*)*, Ispra, Italy*)
(E-mail: daniele.borio@jrc.ec.europa.eu)

The problem of indoor navigation is investigated using a Commercial Off-the-Shelf (COTS) pseudolite system. The system is operated in synchronous and asynchronous mode. It is shown that, when the system is operated in synchronous mode, it is unsuitable for deep indoor operations: in complex propagation environments, the synchronisation required for metre level navigation is difficult to achieve and different solutions have to be adopted. Two asynchronous approaches are thus considered and indoor navigation with metre level accuracy is demonstrated using C/N_0 measurements. The approaches use a modified Receiver Signal Strength (RSS) navigation algorithm and a weighted centroid technique, respectively. In both cases, a pre-filtering stage has been adopted to enhance the quality of C/N_0 measurements. The two methods have been compared under different operating conditions and the advantages and drawbacks of the two techniques have been analysed. The experiments demonstrate that metre level accuracy can be achieved using asynchronous pseudolites. These results are particularly encouraging since they were obtained without exploiting map constraints and prior knowledge of the user position.

KEYWORDS

1. Asynchronous signals. 2. Pseudolite. 3. Received Signal Strength.

Submitted: 9 February 2015. Accepted: 13 October 2015. First published online: 27 November 2015.

1. INTRODUCTION. Indoor navigation using Global Navigation Satellite System (GNSS) signals is a challenging task that involves the solution of several problems such as signal attenuation, fading and measurement biases due to multipath propagation. Although High Sensitivity (HS) techniques allow detecting and tracking weak GNSS signals, indoor navigation based only on GNSS signals seems to be unfeasible and a possible way to fill this gap is the integration with other technologies (Van Diggelen, 2009). Among the technologies developed for indoor GNSS augmentation and navigation, pseudolites or pseudo-satellites (Elrod and Van Dierendock, 1996; Cobb, 1997) have been considered for their ability to provide GNSS-like signals which could be used with minimal receiver changes (Cobb, 1997).

The majority of pseudolite systems exploit the same operational principle of GNSS: all the pseudolites are synchronised to a single time scale and pseudolite signals are used to compute travel times and pseudoranges which are finally used to compute the user position (Söderholm and Jokitalo, 2002).

The development of synchronous systems is however characterised by stringent synchronisation requirements which may lead to significant deployment costs. Moreover, biases in the measurements could still be present due to multipath propagation.

In this paper, the limitations of synchronous pseudolite systems are experimentally investigated using a Commercial Off-the-Shelf (COTS) pseudolite system (Laitinen and Ström, 2009; Space System Finland, 2010). Several tests were performed and different configurations were considered in deep indoor scenarios. Despite significant effort, it was not possible to achieve the synchronisation required for metre level navigation and the limitations of this technology clearly emerged. Although synchronous pseudolite systems can provide good performance in environments such as large hangars and open fields (Laitinen and Ström, 2009), the scenarios considered in this paper are challenging for the technology considered and hence a different approach has to be adopted.

For this reason, two asynchronous approaches have been adapted to pseudolite navigation. The first technique uses Receiver Signal Strength (RSS) measurements (Patwari et al., 2005) and the second is based on the weighted centroid approach (Honkavirta et al., 2009). These techniques are commonly adopted when using WiFi (Honkavirta et al., 2009) and other radio systems (Bekkelien, 2012) for indoor location. Pseudolites are however attractive since pseudolite signals can be processed using the GNSS chip already available in smartphones. In this way, seamless outdoor/indoor navigation can be implemented. This was the original goal of the Japanese Aerospace Exploration Agency (JAXA) for the development of the Indoor MEssaging System (IMES) that will be the indoor extension of the Quasi-Zenith Satellite System (QZSS). IMES exploits the proximity principle that provides a limited accuracy corresponding to the area covered by a single IMES transmitter (Manandhar et al., 2010). In addition to this, pseudolites are natively designed for navigation purposes and their navigation message can be optimised for improving performance. For example, parameters such as the path-loss exponent can be broadcast using the pseudolite signal. This opportunity is not provided by WiFi signals which are used in an opportunistic way for navigation.

Thus one of the main contributions of the paper is the adaptation and empirical analysis of asynchronous navigation approaches for pseudolites. RSS localisation (Tarrio et al., 2008; 2011) is adapted here using the Carrier-to-Noise density power ratio (C/N_0) values estimated by a GNSS receiver processing pseudolite signals. The user position is then determined using a modified Weighted Mean Square Error (WMSE) criterion.

The second method considered is based on the weighted centroid (Wang et al., 2011) where the user position is computed as a weighted mean of the positions of the pseudolites in view.

A pre-filtering stage has been developed and used in both cases to enhance the quality of the C/N_0 measurements. The filter has been designed taking into account the spectral characteristics of the C/N_0 measurements collected in different indoor scenarios.

The analysis has been performed using the COTS pseudolite system mentioned above and detailed in Section 2. Several measurement campaigns were conducted, and the accuracy of the system was assessed using repeatability tests, where the user

https://doi.org/10.1017/S037346331500082X Published online by Cambridge University Press

performed periodic trajectories. The consistency of the different loops performed is used as a quality indicator for the navigation solution obtained. The two methods have been compared under different operating conditions and the advantages and drawbacks of the two techniques have been analysed. The different tests performed and the results obtained are better discussed in Sections 6 and 7. The experiments demonstrate that metre level accuracy can be achieved using asynchronous pseudolites. Moreover, it is shown that the accuracy of the position fixes depends strongly on the geometry defined by the locations of the pseudolites. The results obtained are particularly encouraging, since they were achieved without exploiting map constraints and prior knowledge of the user position. Although the results presented are specific to the scenarios and the technology adopted, the work performed demonstrates the potential of the approach developed. The results obtained are in line with the preliminary findings described in Borio and Gioia (2013) where the authors performed tests using a pseudolite system based on Universal Software Radio Peripherals (USRPs). Despite the different technology adopted for the tests, similar results were obtained.

This work is an extension of a conference paper (Borio and Gioia, 2014) where only preliminary results were presented and weighted centroid positioning was not considered. In this paper, the algorithm adopted for RSS positioning is better detailed and location based on the weighted centroid approach is analysed and used as a term of comparison. Moreover, additional experimental results are provided. The experiments demonstrate that metre level accuracy can be achieved using asynchronous pseudolites.

The reminder of this paper is organised as follows: Section 2 describes the COTS pseudolite system adopted in this work. The limitations of indoor synchronous pseudolite systems are investigated in Section 3 and the asynchronous pseudolite approaches considered for overcoming them are detailed in Section 4. The filter used for enhancing C/N_0 measurements is described in Section 5 along with the spectral analysis performed for the filter design. The experimental setup and the tests performed are described in Section 6. Experimental results are detailed in Section 7 and, finally, Section 8 concludes the paper.

2. PSEUDOLITE NAVIGATION SYSTEM.

In this section, the characteristics of the COTS pseudolite system (Laitinen and Ström, 2009; Space System Finland, 2010) used for the analysis are briefly summarised. In particular, the pseudolite system adopted is made of:

- Six pseudolites operating in the Global Positioning System (GPS) L1 band and able to broadcast continuous and pulsed signals. Each pseudolite can be operated in synchronous or asynchronous mode.
- A Master Control Station (MCS) along with a software tool able to coordinate and to synchronise the different pseudolites computing the synchronisation parameters for the different devices. The MCS is not required when the system is operated in asynchronous mode.
- Radio modems used for the communication between the components of the system.
- Two modified GPS receivers able to process pseudolite signals. One of the receivers is used as reference by the MCS to determine synchronisation parameters.

https://doi.org/10.1017/S037346331500082X Published online by Cambridge University Press

The receivers are modified to support non-standard GPS Coarse Acquisition (C/A) Pseudo-Random Noise (PRN) codes. These codes can be allocated to pseudolite signals.

The system is able to provide signals with the same format as that of GPS L1 C/A signals and the MCS can synchronise the system to the GPS time scale. The MCS synchronises the different nodes of the system exploiting the knowledge of distances of the different pseudolites with respect to the reference receiver. Moreover, a good synchronisation is possible only if the MCS have all the pseudolites in Line-Of-Sight (LOS) conditions. It this way, the pseudoranges determined from the different pseudolites can be used to compute synchronisation errors. The MCS software performs several checks to verify the synchronisation level. If the checks are not passed, the synchronisation process is restarted without achieving even partial results.

When operated singularly, pseudolites can be adopted for asynchronous navigation using, for example, the approaches described in Section 4.

3. LIMITATIONS OF SYNCHRONOUS SYSTEMS.

In this section, the limitations of the synchronous pseudolite system considered are analysed in light of experiments conducted in indoor environments.

The first limitation is that the MCS has to have all the pseudolites in LOS in order to accurately measure the pseudoranges of the different pseudolites and compare them with the actual distances stored in the MCS control software. As discussed in Section 2, the MCS sends control signals to the pseudolites which adjust their local clocks in order to match the pseudoranges measured by the MCS to the actual distances. Thus multipath and other propagation errors have to be sufficiently small to achieve synchronisation. Note that range measurements can be corrupted by significant biases (Conti et al., 2012) depending on the environment considered. In the indoor scenarios analysed in this work, the propagation conditions did not allow the MCS to achieve the synchronisation level required.

In order to overcome limitations connected to the MCS and analyse measurement errors, a relative positioning approach was implemented using two u-blox LEA-6 T GPS devices which were used as reference and rover receivers, respectively. Pseudorange measurements from the two receivers can be modelled as

$$\begin{aligned} \rho_{rov,i} &= d_{rov,i} + b_{rov} + b_{pl,i} + \eta_{rov,i} \\ \rho_{ref,i} &= d_{ref,i} + b_{ref} + b_{pl,i} + \eta_{ref,i} \end{aligned} \tag{1}$$

where $d_{rov,i}$ and $d_{ref,i}$ are the geometric distances between rover/reference receivers and the ith pseudolite. b_{rov} and b_{ref} are the clock biases of the rover and reference receivers and $b_{pl,i}$ is the clock bias of the ith pseudolite. $b_{pl,i}$ is a synchronisation error specific to each pseudolite. $\eta_{rov,i}$ and $\eta_{ref,i}$ are residual unmodelled errors. The synchronisation error, $b_{pl,i}$, can be removed considering single pseudorange differences:

$$\begin{aligned} \Delta\rho_i &= \rho_{rov,i} - \rho_{ref,i} \\ &= d_{rov,i} - d_{ref,i} + b_{rov} - b_{ref} + \eta_{rov,i} - \eta_{ref,i} \end{aligned} . \tag{2}$$

https://doi.org/10.1017/S037346331500082X Published online by Cambridge University Press

Finally, using the geometric distance between the reference receiver and the ith pseudolite, it is possible to construct new measurements free of pseudolite synchronisation errors:

$$\bar{\rho}_i = \Delta\rho_i + d_{ref,i} = d_{rov,i} + \Delta b + \Delta\eta_i \tag{3}$$

where $\Delta b = b_{row} - b_{ref}$ and $\Delta\eta_i = \eta_{rov,i} - \eta_{ref,i}$. Note that Equation (3) has the same functional form of the pseudoranges adopted for GNSS positioning (Kaplan and Hegarty, 2005) and in particular a single clock bias term, Δb, is present. This term is common to all the pseudolite measurements and can be estimated by adding it as an unknown in the navigation solution. This is the same principle adopted by commercial GNSS receivers.

Note that the principle described above is valid only if the reference and rover receivers are accurately synchronised, i.e., if their measurements are generated and time-tagged using the same time reference. This is a stringent requirement and represents an additional limitation of indoor synchronous pseudolite navigation systems. In order to achieve precise receiver synchronisation, two methodologies were adopted. In the first case, a specific pseudolite, named Master Pseudolite (MPL), was turned on before all the other elements of the network. Additional pseudolites were activated only after reference and rover receivers used the MPL signal for the measurement generation and time-tagging. Alternatively, when the receivers were able to determine a position fix using GPS, GPS time was adopted.

Despite these efforts, it was not possible to compute valid position fixes employing the measurements generated using Equation (3). The problem was investigated considering double pseudorange differences

$$\nabla\Delta\rho_{i,j} = \bar{\rho}_i - \rho_j. \tag{4}$$

The scenario where the measurements were taken, i.e., the meeting room described in Section 6.1, was also simulated assuming perfect receiver synchronisation. Measured and simulated double pseudorange differences are shown in Figure 1. In both simulated and real tests, the user is repeating the same rectangular trajectory: for this reason double differences oscillate periodically. From Figure 1, it can be noted that real measurements are affected by biases that are difficult to estimate. This effect is probably due to a lack of synchronisation between reference and rover receivers: synchronisation errors affect measurement generation and time-stamping. This lack of synchronisation can be due to multipath and other indoor propagation effects.

The residual bias on the measurements has been further studied considering a zero-baseline configuration. In particular, reference and rover receivers were kept static in a zero-baseline configuration for 60 seconds before starting the dynamic test. The measurements obtained during the first phase of the test were used to estimate the biases from the measurements. However, when the rover receiver started moving, the measurement corrections were no longer valid and the position solution computed started diverging. This fact is clearly shown in Figure 2, which shows the position solution obtained using pseudorange measurements corrected for the initial synchronisation biases. These results indicate that synchronisation biases are time-varying and depend on the user dynamics. For this reason, synchronous pseudolite systems can not be easily used in deep indoor environments.

4. ASYNCHRONOUS PSEUDOLITE POSITIONING.

The two asynchronous navigation approaches considered are detailed below.

https://doi.org/10.1017/S037346331500082X Published online by Cambridge University Press

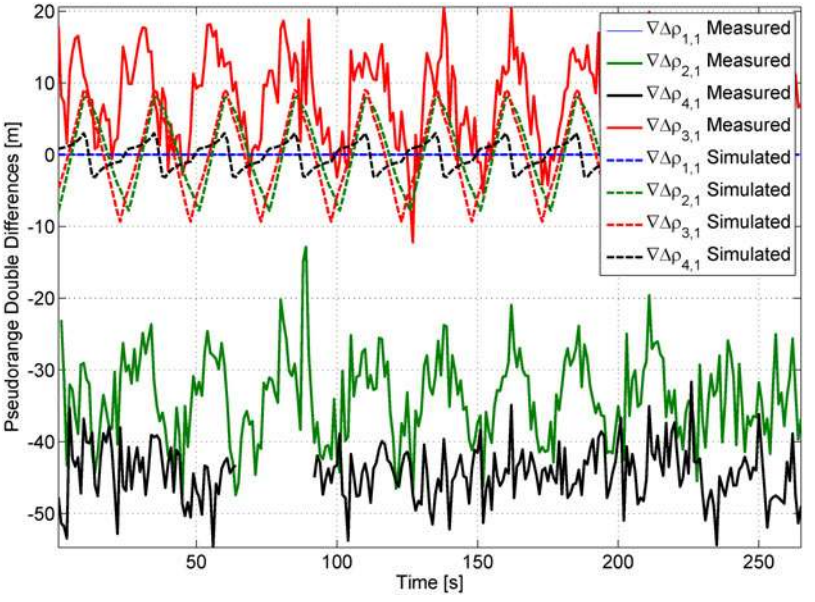

Figure 1. Double pseudorange differences computed from the measurements collected from the four pseudolites using two u-blox LEA 6-T receivers.

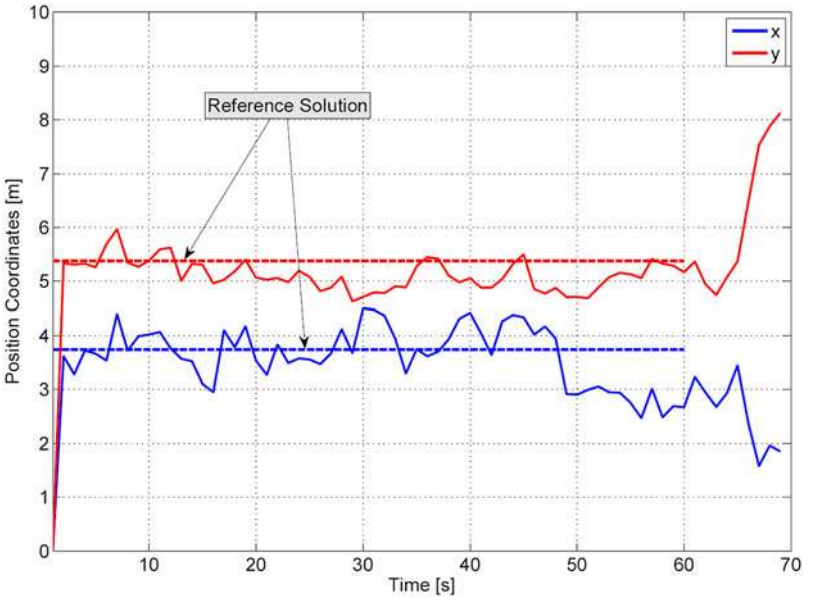

Figure 2. Position solution obtained using corrected pseudorange measurements where initial synchronisation biases were removed exploiting the zero-baseline configuration adopted during the first 60 seconds of the test. When the rover receiver starts moving, the measurement corrections become invalid and the position solution starts diverging.

https://doi.org/10.1017/S037346331500082X Published online by Cambridge University Press

4.1. *RSS positioning.* According to Patwari et al. (2005), RSS is defined as the voltage measured by a receiver's Receiver Signal Strength Indicator (RSSI) circuit and corresponds to the received power measured on a logarithmic scale. RSS measurements are usually modelled as (Okumura et al., 1968; Lindström et al., 2007; Fontanella et al., 2012; Patwari et al., 2005):

$$P(d) = P_0 - 10\alpha \log_{10} \frac{d}{d_0} \tag{5}$$

where $P(d)$ is the RSS measured at the distance d from the emitter. α is the path-loss exponent and P_0 is the power received at a short reference distance, d_0.

RSS-based techniques are widely used because RSS is easy to measure. In particular, RSS values can, for example, be obtained from the Automatic Gain Control (AGC) levels (Scott, 2011; Isoz et al., 2010; Lindström et al., 2007) or C/N_0 measurements (Kraemer et al., 2012).

In this paper, C/N_0 measurements are adopted for RSSI positioning. In particular, Equation (5) can be rewritten in terms of C/N_0 measurements as

$$\left(\frac{C}{N_0}\right)_i = K_i - \alpha 10 \log_{10}(d_i) \tag{6}$$

where the index i has been introduced to denote C/N_0 measurements from the i^{th} transmitter and K_i is a constant accounting for the power of the i^{th} transmitted signal and for the reference distance d_0. Unless specified, the C/N_0 will always be expressed in units of dB-Hz.

When the constants K_i and α are known, it is possible to establish a direct relationship between the measured C/N_0 and the transmitter-receiver distance. In turn, distances can be expressed as a function of the user position:

$$d_i = \sqrt{(x_u - x_i)^2 + (y_u - y_i)^2} \tag{7}$$

where (x_u, y_u) and (x_i, y_i) are the coordinates of the user and the i^{th} pseudolite, respectively.

Although Equation (7) considers the case of 2D positioning, the 3D case can be easily obtained. Using Equation (7), it is possible to rewrite Equation (6) as

$$\left(\frac{C}{N_0}\right)_i = K_i - \frac{1}{2}\alpha 10 \log_{10}\left[(x_u - x_i)^2 + (y_u - y_i)^2\right] \tag{8}$$

where the user coordinates are the only unknowns. When a sufficiently large number of C/N_0 measurements is available ($N \geq 2$), it is possible to determine the user position for example by minimising the following cost function:

$$J(x, y) = \sum_{i=0}^{N-1} E_i^2 \tag{9}$$

where

$$E_i = \left(\frac{C}{N_0}\right)_i - K_i + \frac{1}{2}\alpha 10 \log_{10}\left[(x - x_i)^2 + (y - y_i)^2\right] \tag{10}$$

is the error between the measured C/N_0 and empirical model in Equation (8). In this way, the user coordinates are obtained as

$$(x_u, y_u) = \arg\min_{x,y} J(x, y). \tag{11}$$

https://doi.org/10.1017/S037346331500082X Published online by Cambridge University Press

Cost function in Equation (9) is the Mean Square Error (MSE) between the measured C/N_0 values and the model in the right-hand side of Equation (8). The minimisation problem in Equation (11) can be solved using a gradient descent algorithm where the initial user position can be set equal to the average of the pseudolite coordinates. The MSE algorithm detailed above was tested using the C/N_0 measurements collected in several indoor environments. However, it has been empirically verified that as C/N_0 values approach zero, significant errors are introduced. C/N_0 measurements do not only carry distance information but are also indicators of the signal quality. Thus low C/N_0 measurements should be considered unreliable. In the limit case, measurements with C/N_0 values close to zero should be removed. For this reason, cost function in Equation (9) was modified to de-weight measurements characterised by low C/N_0 values. The new cost function adopted is defined as:

$$J_w(x,y) = \sum_{i=0}^{N-1} \left(\frac{C}{N_0}\right)_i E_i^2 \tag{12}$$

where the subscript "w" has been added to denote the fact that the cost function is now a form of WMSE where each term in the summation in Equation (12) is weighted by its relative C/N_0. In Equation (12), $(C/N_0)_i$ is the C/N_0 of the i^{th} received pseudolite signal expressed in dB-Hz.

In Equation (12) the different errors are weighted proportionally to the C/N_0. Other weighting functions can be adopted and their analysis is left for future work.

The WMSE algorithm significantly outperforms the MSE method defined by cost function in Equation (9) and, for this reason, only results obtained minimising Equation (12) are presented in Section 7.

The approach detailed above assumes the knowledge of the parameters

$$\alpha, K_i \quad \text{for } i = 0, \ldots, N-1. \tag{13}$$

These parameters are however unknown and have to be determined using a calibration process. This process was performed using C/N_0 measurements collected in known positions. Additional details on the calibration procedure adopted for determining parameters in Equation (13) can be found in (Gioia, 2014).

Using this approach, it was finally possible to perform indoor location using C/N_0 measurements. In the experiments detailed below, C/N_0 measurements were obtained from a u-blox LEA-6 T receiver which provides them in a dedicated message. Although different algorithms are available for the estimation of the C/N_0 (Pini et al., 2008), the approach used by the u-blox receiver is not publically available. This is not a limitation for the RSS algorithm adopted which does not rely on specific techniques for the generation of C/N_0 measurements. The measurements are provided with a 1 Hz sampling rate. This rate is commonly adopted by commercial GPS receivers and it is the default setting for the u-blox device.

4.2. *Weighted Centroid positioning.* In the weighted centroid approach, the user position is determined as a linear combination of the pseudolite coordinates:

$$P_u = (x_u, y_u) = \frac{\sum_{i=0}^{N-1} w_i P_{pl,i}}{\sum_{i=0}^{N-1} w_i} \tag{14}$$

https://doi.org/10.1017/S037346331500082X Published online by Cambridge University Press

where

$$P_{pl,i} = (x_i, y_i)$$

is the vector containing the coordinates of the ith pseudolite and w_i is a weight determined from the C/N$_0$ of the ith received pseudolite signal. In this work, the following relationship is adopted

$$w_i = 10^{(C/N_0)_i/10} \tag{15}$$

Equation (15) defines a transformation from the C/N$_0$ measurements to the position/range domain. In particular, when a standard GNSS receiver is adopted, the user position is computed using pseudorange measurements expressed in metres. The variance of such pseudoranges is proportional to the weights defined by Equation (15) (Kuusniemi et al., 2007) and it is used in classical Weighted Least Squares (WLS) to compute the user position. Similarly, the weighting Equation (15) has been adopted here for weighing the different pseudolite positions.

5. PRE-FILTERING TECHNIQUES. In order to improve the performance of asynchronous positioning algorithms using C/N$_0$ measurements, a pre-filtering stage was introduced. In particular, filters were designed exploiting the frequency and correlation properties of C/N$_0$ measurements. Note that C/N$_0$ measurements are characterised by a Direct Current (DC) component that is determined by the average received power and the noise floor. The DC components of the C/N$_0$ measurements define a geometric point that can be thought as a reference location with respect to which the user is moving (Borio and Gioia, 2014). For the analysis, the DC terms have been removed in order to better study the characteristics of the zero mean components that determine the relative displacement of the user.

In Borio and Gioia (2014), the Power Spectral Densities (PSDs) of C/N$_0$ measurements were studied for the meeting room test described in Section 6.1. It was shown that the PSD are characterised by a main peak at about 0·031 Hz corresponding to a periodicity of about 32 s, the average time required by the user to perform a loop. In addition to this, most of the power was significantly attenuated for frequencies higher than 0·15 Hz. This fact suggests that high frequency components can be removed with a cut-off frequency $f_c = 0.15$ Hz. This result is confirmed by Figure 3 that shows the PSD of the measurements from the five pseudolites used in the corridor test described in Section 6.2.

The power of the C/N$_0$ measurements is mainly concentrated in the low frequencies and thus the quality of C/N$_0$ measurements can be improved by using a low-pass filter. In addition to the considerations derived from the PSD analysis, the following requirements have been identified for the filter design:

- The filter should have a short impulse response: C/N$_0$ measurements are time-varying and long impulse responses may introduce significant biases due to the averaging of signals which are only locally stationary. The requirement of having short impulse responses limits the delay introduced by the filter.
- It has been empirically verified (Borio and Gioia, 2014) that symmetric impulse responses provide better results and thus should be adopted.

https://doi.org/10.1017/S037346331500082X Published online by Cambridge University Press

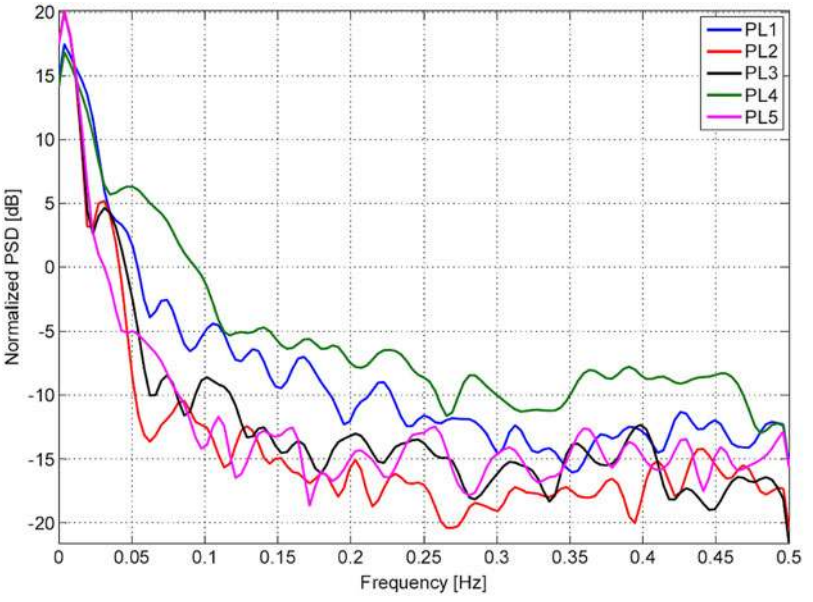

Figure 3. Normalised PSDs of the C/N_0 measurements obtained in the corridor test described in Section 6.2. The PSDs have been normalised in order to have signals with unitary power.

The results discussed in Borio and Gioia (2014) and the findings reported above have been used to design a Finite Impulse Response (FIR) Wiener filter for the pre-processing of C/N_0 measurements. The Transfer Function (TF) of the filter is depicted in Figure 4 along with its impulse response. The filter mainly preserves low frequency components as desirable from the PSD analysis. The short impulse response selected (seven samples) is sufficient to significantly improve the algorithm performance, as detailed in Section 7, without introducing significant delays.

By inspecting the impulse response of the Wiener filter, it was found that it can be effectively approximated by a triangular function. This fact is highlighted in Figure 4 where the impulse responses and TFs of the two filters are compared. Their good agreement suggests the usage of a filter with a triangular impulse response that is simpler to design for different filter lengths.

The effect of pre-filtering can be clearly seen in Figure 5 which shows filtered and unfiltered C/N_0 measurements. High-frequency noise components are effectively removed by the pre-filtering stage. The measurements are from pseudolite 2 in the corridor test.

6. EXPERIMENTAL SETUP.

The effectiveness of the asynchronous pseudolite approaches considered in this paper was tested under different conditions. In the following, two of the deep-indoor scenarios considered for the analysis are described. The environments selected are from an office building and are scenarios typically considered for network localisation (Conti et al., 2012).

6.1. *Large Meeting Room.*

The first scenario considered was the large meeting room of about 5 m × 10 m shown in Figure 6. Four pseudolites were placed in the

https://doi.org/10.1017/S037346331500082X Published online by Cambridge University Press

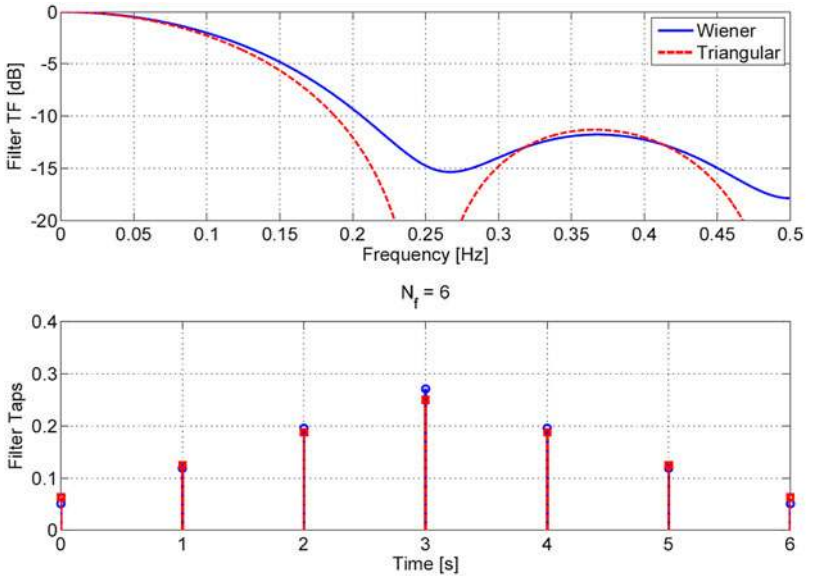

Figure 4. TFs and impulse responses of the filters used to pre-process C/N_0 measurements.

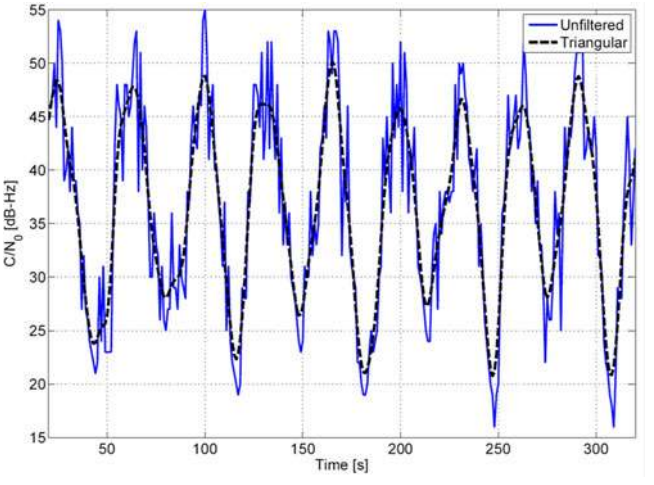

Figure 5. Impact of triangular filtering on C/N_0 measurements. High-frequency noise components are effectively removed by the pre-filtering stage. Measurements are from pseudolite 2 in the corridor test.

corners of the room. The positions of the pseudolites were carefully surveyed and used for the computation of the user position. Two types of experiments were conducted:

- *Repeatability tests*: the user performed several loops around the large table present in the meeting room trying to always repeat the same trajectory. The quality of the

https://doi.org/10.1017/S037346331500082X Published online by Cambridge University Press

Figure 6. Different views of the large (5 m × 10 m) meeting room used for testing asynchronous pseudolite approaches. Four pseudolites were placed in the corners of the room.

navigation solution is assessed by comparing the different trajectories estimated for the different loops. A high consistency level of the navigation solution indicates good performance of the system.

- *Control point experiments*: several control points were placed in the meeting room. The locations of the control points were carefully determined by surveying the room. For each control point data were collected and used for calibration purposes.

Experimental results obtained for repeatability tests are provided in Section 7 whereas details on the calibration procedure and on control point experiments can be found in Gioia (2014).

6.2. *Corridor Scenario.* The performance of the asynchronous pseudolite system was further tested considering a user moving along the corridor of the second floor of the building depicted in Figure 7. In this case, five pseudolites were adopted and placed according to the geometry shown in Figure 7. It is noted that the building where the tests were performed has a geometry mainly oriented along the North-South direction. Consequently, the five pseudolites are able to provide useful information mainly for the estimation of the North coordinate. The geometry along the East-West direction is quite poor due to the pseudolite displacement, which is less than 10 m.

7. EXPERIMENTAL RESULTS. This section presents the results obtained using the asynchronous pseudolite systems described in Section 4. The different solutions are compared and the effects of pre-filtering are evaluated. The impact of filtering is at first evaluated for the meeting room scenario.

7.1. *Large Meeting Room Test.* In the test considered, the user performed five loops around a large table present in the meeting room described in Section 6.1 trying to always repeat the same trajectory. RSS positioning is presented at first. A comparison between the solutions obtained applying triangular (red dashed line) and Wiener (blue line) filtering is provided in Figure 8. The solution using unfiltered

https://doi.org/10.1017/S037346331500082X Published online by Cambridge University Press

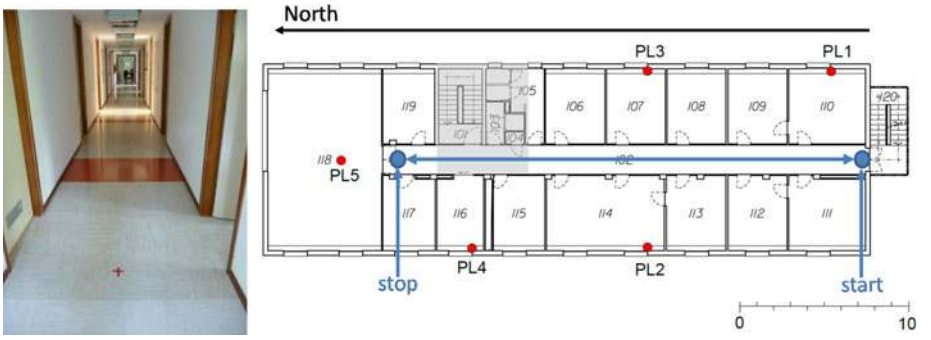

Figure 7. Location of the five pseudolites used for the corridor experiment. The blue line indicates the trajectory performed during the experiment detailed in Section 7.2.

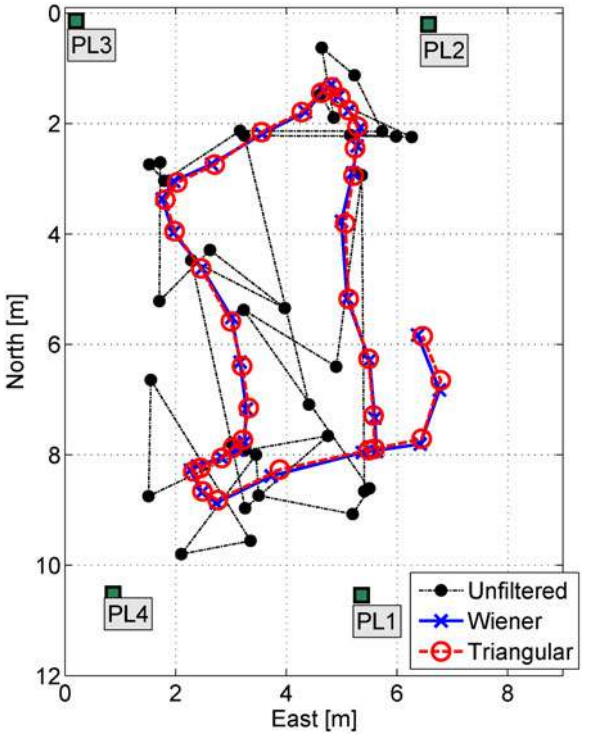

Figure 8. Comparison between navigation solutions obtained using RSS positioning and different pre-filtering stages for the C/N_0 measurements. Loop performed in a large meeting room.

measurements is also plotted (black dashed line) to evaluate the effects of the filters. In order to have a clear representation only one loop is plotted in Figure 8. The position solutions are presented in a local frame centred in the corner of the room closed to pseudolite 3.

https://doi.org/10.1017/S037346331500082X Published online by Cambridge University Press

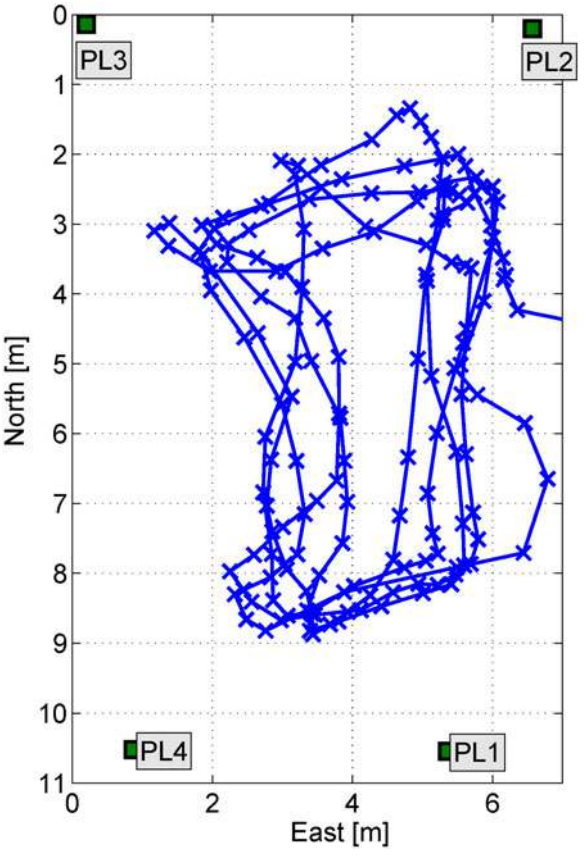

Figure 9. Position estimates obtained using the RSS asynchronous technique proposed and processing filtered C/N_0 measurements. Triangular filter, repeatability tests.

From Figure 8, the benefits of filtered C/N_0 measurements clearly emerge: although the unfiltered solution (black line) is contained within the room, it is not possible to identify the trajectory followed by the user. On the contrary, the user trajectory can be easily identified when filtered measurements are used. The two filtering techniques considered provide similar performance and no significant differences can be noted. Since the performance obtained with the two filters is very similar, the triangular filter should be preferred for its simplified design and implementation.

The quality of the navigation solution is assessed in Figure 9 by comparing the trajectories estimated for the different loops. The position solutions have been obtained using the RSS approach and filtered measurements (triangular filter). From Figure 9, a high consistency level of the navigation solution emerges: only sub-metre differences can be appreciated between different loops. This indicates the good performance of the system.

The analysis performed using the RSS approach has been repeated using the weighted centroid approach: the navigation solutions obtained using this method are plotted in Figures 10 and 11. From Figure 10, the improvement due to pre-filtering

https://doi.org/10.1017/S037346331500082X Published online by Cambridge University Press

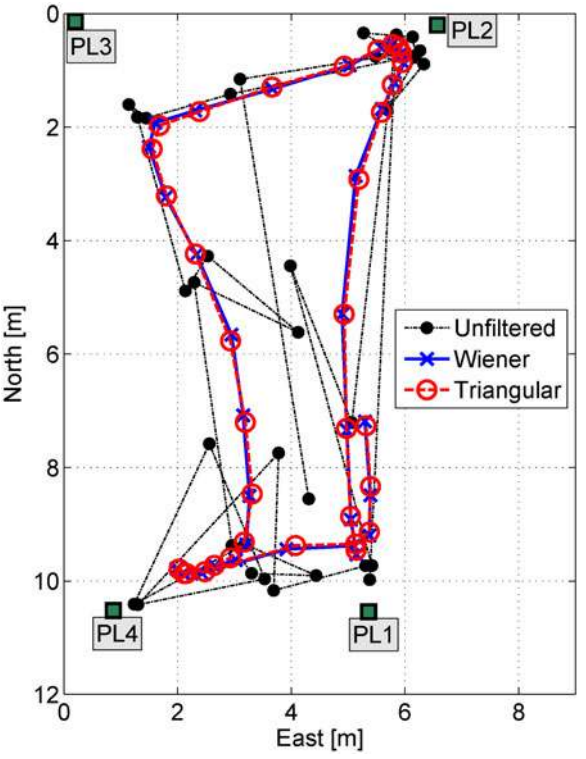

Figure 10. Comparison between navigation solutions obtained using weighted centroid positioning and different pre-filtering stages for the C/N_0 measurements. Loop performed in a large meeting room.

also clearly emerges for the weighted centroid case. This supports the findings obtained using the RSS approach and confirms the benefits of pre-filtering: only when filtered measurements are employed can the user trajectory be easily identified.

As for the RSS case, only the position solutions obtained using the triangular filter are considered in Figure 11. Also in this case, a high consistency of the navigation solution clearly emerges, demonstrating the good performance achievable using this approach.

From Figure 11, it also emerges that the weighted centroid approach constrains the navigation solution to lay within the polygon described by the pseudolites. This is due to the fact that weights from Equation (15) are always positive. This could be considered an advantage for indoor navigation when the pseudolites are placed in the corners or along the sides of the structure inside which the user is moving. This property can be exploited to constrain the user position within the building or room of interest.

Although the lack of a reference trajectory makes it difficult to directly compare the position solutions depicted in Figures 9 and 11, the weighted centroid seems to provide improved performance. In particular, the user was trying to perform a trajectory as close as possible to the walls of the room. The only exception was along the side between pseudolite 3 and pseudolite 4 where the presence of a large bookcase was

https://doi.org/10.1017/S037346331500082X Published online by Cambridge University Press

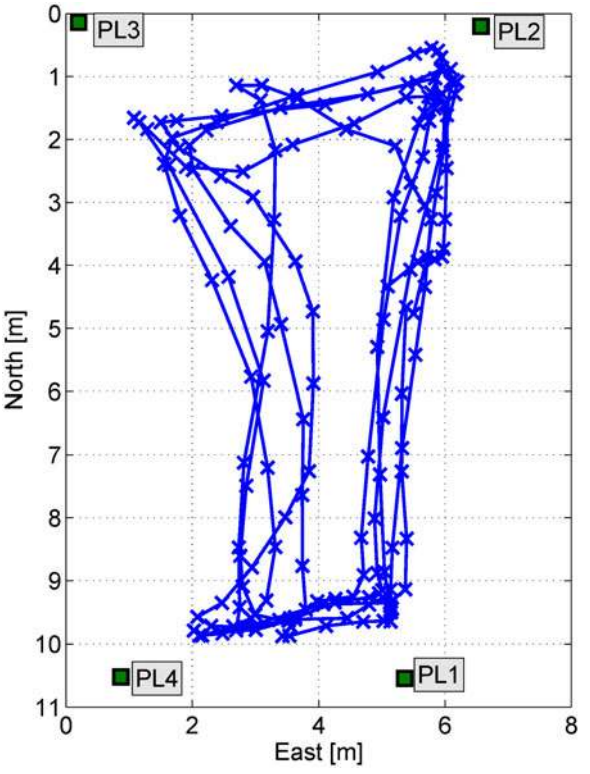

Figure 11. Position estimates obtained using the weighted centroid technique and processing filtered C/N_0 measurements. Triangular filter, repeatability tests.

forcing a trajectory slightly displaced towards the centre of the room. The solutions obtained using the weighted centroid seem to provide a more faithful representation of the user motion.

7.2. *Corridor Scenario.* In the second scenario, the user performed a periodic trajectory moving between the beginning and the end of the corridor depicted in Figure 7. In particular, the user was moving back and forth along the blue line depicted in Figure 7. As for the previous experiment, the user performed five loops. The position solutions have been computed in a local frame centred on pseudolite 1.

The North and East coordinates of the position solutions estimated using the aforementioned asynchronous approaches are provided in Figure 12. Although the loops can be clearly identified from the North component depicted in the upper box of Figure 12, an anomalous behaviour can be clearly seen in correspondence of the shaded areas reported in the figure.

The trajectory in the shaded area shows an almost constant North component while the user was moving with an almost constant velocity. Such an anomaly is consistent in all loops performed and occurred in correspondence to the shaded area in Figure 7. In this area, there is the entrance of the floor and a direct view on the stairs of the building. This can cause a change in the propagation conditions and compromise the effectiveness of the position solution. The East component is more degraded by this effect as

https://doi.org/10.1017/S037346331500082X Published online by Cambridge University Press

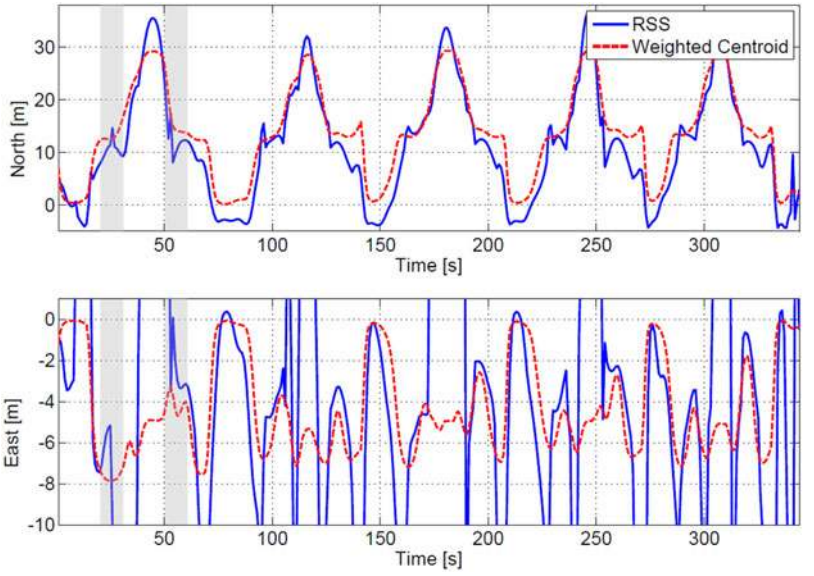

Figure 12. North and East coordinates of the position solutions estimated using asynchronous approaches for the corridor experiments. An anomalous behaviour has been identified in the middle of the corridor. Comparison between RSS and weighted centroid positioning.

clearly seen in the bottom part of Figure 12. This fact is justified by the geometry defined by the pseudolite location.

The trajectory obtained for the RSS and weighted centroid techniques are further analysed in Figure 13 where the North and East components shown in Figure 12 are jointly plotted in the horizontal plane.

Figure 13 confirms the results shown in Figure 12, i.e., the errors are mainly along the East component of the trajectory performed. As already highlighted, this phenomenon is mainly due to geometric effects: the building concerned has an elongated shape and offices are placed symmetrically along the central corridor of about 36 metres. The pseudolites were placed in different offices and a poor geometry was obtained along the direction perpendicular to the central corridor. For this reason, the East component of the position solution is severely penalised, most of all in the RSS case. The weighted centroid is significantly more robust to propagation anomalies as clearly emerges from Figures 12 and 13. The geometrical property discussed above allows one to constrain the position solutions within the building.

Finally, it is possible to note that weighted centroid positioning can degenerate to a form of proximity-based navigation when a received signal is significantly stronger than the others. This fact clearly emerges in Figure 13, for example when the user is close to pseudolite 1. In this case, the signal received is two orders of magnitude stronger than the others and the user position is determined as that of pseudolite 1. For this reason, the East component assumes a value close to zero, the coordinate of pseudolite 1. The user was however in the centre of the corridor with East coordinate approximately equal to -6 metres as in the rest of the trajectory reported in Figure 12. This problem can be solved by placing pseudolites in a symmetrical way. From Figure 13

https://doi.org/10.1017/S037346331500082X Published online by Cambridge University Press

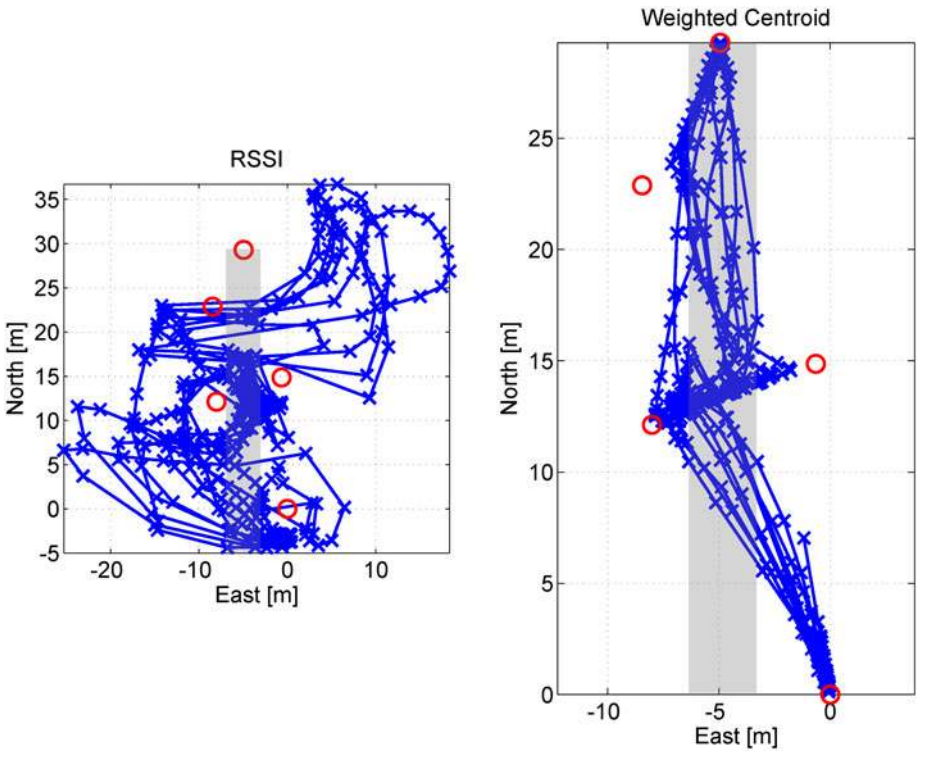

Figure 13. Position estimates obtained using the RSS and weighted centroid techniques for the corridor tests. Red circles represent the positions of the pseudolites. An anomalous behaviour is observed along the East component.

it also emerges that the East error for RSS positioning can be as large as 25 metres. The error is limited to about 3 metres for weighted centroid positioning.

8. CONCLUSIONS. In this paper, the problem of indoor navigation using pseudolites was considered. Synchronous and asynchronous approaches were at first analysed and potential limitations of synchronous pseudolite systems in indoor scenarios were identified. In particular, the synchronous system adopted for the experiments was not able to cope with the harsh propagation conditions considered. Although two different approaches were adopted to obtain synchronous Time Of Arrival (TOA) measurements, the level of synchronisation required for indoor navigation was never achieved. Although the analysis performed highlights potential limitations of synchronous pseudolite systems in harsh propagation conditions, different approaches can be adopted to address the synchronisation problem. The limitations discussed are related to the system adopted and better performance may be obtained using more sophisticated synchronisation approaches. For example, a shared clock connected through wires to the different pseudolites can be used.

In order to overcome the limitations of the system considered, two asynchronous localisation approaches were adapted to pseudolites and used for indoor navigation. The

https://doi.org/10.1017/S037346331500082X Published online by Cambridge University Press

two techniques use C/N_0 measurements from different pseudolites to compute the user position. The first approach is based on the RSS principle and on an empirical model that allows mapping received C/N_0 values into distances. The second technique determines the user position as the weighted centroid of the pseudolite locations using C/N_0 measurements for determining the different weights. Both techniques enable indoor navigation with metre level accuracy that was demonstrated in different indoor environments. It was also shown that the performance of an asynchronous system can be greatly improved using a pre-filtering stage for smoothing C/N_0 measurements. The use of asynchronous pseudolites significantly reduces the design and implementation constraints of the system because the different devices can operate independently. Moreover, the system can be implemented in frequency bands different from the GNSS frequencies since inter-frequency biases are no longer relevant. Among the approaches analysed, weighted centroid location is the most robust to unmodelled phenomena and should be preferred also because it does not need a calibration phase.

ACKNOWLEDGMENTS

This work has been partially supported by the European Commission in the framework of the EPCIP 2010 project (C.32253-2011 NFP – AWP CIPS 2010). The tests conducted for this work were performed in the GPS L1 frequency band solely in order to reduce the development time and to exploit GNSS receivers available on the market. Other frequencies can be adopted for this type of operation.

REFERENCES

Bekkelien, A. (2012). Bluetooth Indoor Positioning, Master Thesis, University of Geneva, http://tam.unige.ch/assets/documents/masters/bekkelien/Bekkelien_Master_Thesis.pdf, March

Borio, D. and Gioia, C. (2013). Indoor Navigation Using Asynchronous Pseudolites *Proceedings of the 6th European Workshop on GNSS Signals and Signal Processing*, Munich, Germany, 5–6

Borio, D. and Gioia, C. (2014). Improved pseudolite navigation using C/N_0 measurements *Proceedings of the 22nd European Signal Processing Conference (EUSIPCO)*, Lisbon, Portugal, September.

Cobb, H.S. (1997). GPS pseudolites: Theory, design and applications, PhD Thesis, Stanford University, http://waas.stanford.edu/wwu/papers/gps/PDF/Thesis/StuCobbThesis97.pdf, September.

Conti, A., Guerra, M., Dardari, D., Decarli, N. and Win, M.Z. (2012). Network experimentation for cooperative localization. *IEEE Journal on Selected Areas Communication*, **30**(2), 467–475.

Elrod, B.D. and Van Dierendonck, A.J. (1996), *Pseudolites* in *Global Positioning System, Theory and Applications*. American Institute of Aeronautics and Astronautics (AIAA), 2(2), 51–79.

Fontanella, D., Bauernfeind, R. and Eissfeller, B. (2012). In-car GNSS jammer localization with a vehicular ad-hoc network. *Proceedings of the 25th International Technical Meeting of The Satellite Division of the Institute of Navigation ION/GNSS*. Nashville, TN, pages 2885–2893, September.

Gioia, C. (2014). GNSS navigation in difficult environments: Hybridization and reliability. PhD Thesis, University Parthenope of Naples, http://pang.uniparthenope.it/sites/default/files/PhD_thesis_CG.pdf.

Honkavirta, V., Perala, T., Ali-Loytty, S. and Piche, R. (2009). A comparative survey of WLAN location fingerprinting methods, *Proceedings of the 6th Workshop on Positioning, Navigation and Communication (WPNC)*, Hannover, Germany, pp 243–251.

Isoz, O., Balaei, A.T. and Akos, D. (2010). Interference detection and localization in the GPS l1 band. *Proceedings of the International Technical Meeting of The Institute of Navigation (ITM/ION)*, San Diego, CA, pages 925–929.

Kaplan, E.D. and Hegarty, C. (2005). Understanding GPS: Principles and Applications. 2nd edition, *Artech House*.

Kraemer, I., Dykta, P., Bauernfeind, R. and Eissfeller, B. (2012). Android GPS jammer localizer application based on C/N_0 measurements and pedestrian dead reckoning. *Proceedings of the 25th International*

Technical Meeting of The Satellite Division of the Institute of Navigation ION/GNSS, Nashville, OR, pages 3154–3162.

Kuusniemi, H., Wieser, A., Lachapelle, G. and Takala, J. (2007). User-level reliability monitoring in urban personal satellite-navigation. *IEEE Transactions on Aerospace and Electronic Systems*, **43**(4), 1305–1318.

Laitinen, H. and Ström, M. (2009). Single-frequency carrier navigation in a synchronised pseudolite network. *Proceedings of the European Navigation Conference ENC-GNSS*, pages 1–8, Naples, Italy.

Lindstrom, J., Akos, D.M., Isoz, O. and Junered, M. (2007). GNSS interference detection and localization using a network of low cost front-end modules. *Proceedings of the 20th International Technical Meeting of the Satellite Division of The Institute of Navigation ION/GNSS*, Fort Worth, TX, pages 1165–1172 September.

Manandhar, D., Kawaguchi, S. and Torimoto, H. (2010). Results of IMES (indoor messaging system) implementation for seamless indoor navigation and social infrastructure platform. *Proceedings of the 23rd International Technical Meeting of the Satellite Division of The Institute of Navigation*, pages 1184–1191, Portland, OR, September.

Okumura, Y., Ohmori, E., Kawano, T. and Fukuda, K. (1968). Field strength and its variability in vhf and uhf land-mobile radio service. *Review of the Electrical Communication Laboratory*, **16**(9–10), 825–873.

Patwari, N., Ash, J., Kyperountas, S., Hero, A., III, Moses, R.L. and Correal, N.S. (2005). Locating the nodes: cooperative localization in wireless sensor networks. *IEEE Signal Processing Magazine*, **22**(4), 54–69.

Pini, M., Falletti, E. and Fantino, M. (2008). Performance Evaluation of C/N_0 Estimators Using a Real Time GNSS Software Receiver. *Proceedings of the 10th IEEE International Symposium on Spread Spectrum Techniques and Applications (ISSSTA)*, Bologna, Italy, pages 28–31, 25–28 August.

Scott, L. (2011). J911: The case for fast jammer detection and location using crowdsourcing approaches. *Proceedings of the 24th International Technical Meeting of The Satellite Division of the Institute of Navigation ION/GNSS*, Portland, OR, pages 1931–1940, September.

Söderholm, S. and Jokitalo, T. (2002). Synchronized pseudolites – the key to indoor navigation. *Proceedings of the International Technical Meeting of the Satellite Division of the Institute of Navigation (ION GPS)*, Portland, OR, pages 24–27, September.

Space System Finland. (2010). User's Manual Pseudolite Navigation System, March.

Tarrio, P., Bernardos, A.M. and Casar, J. (2011). Weighted least squares techniques for improved received signal strength based localization, *Sensors*, **11**, 8569–8592.

Tarrio, P., Bernardos, A.M., Besada, J. and Casar, J. (2008). A new positioning technique for RSS-based localization based on a weighted least squares estimator. *Proceedings of the IEEE International Symposium on Wireless Communication Systems (ISWCS)*, pages 633–637.

Van, Diggelen, F. (2009). A-GPS: Assisted GPS, GNSS, and SBAS, 1st edition, GNSS Technology and Applications Series. *Artech House*, March.

Wang, J., Urriza, P., Han, Y. and Cabric, D. (2011). Weighted centroid localization algorithm: Theoretical analysis and distributed implementation. *IEEE Transaction on Wireless Communication*, **10** (10), 3403–3413.